Numerical Solutions of Differential Equations using Neural Networks

Candidate Number: 1090497

1 Introduction

In recent years, neural networks have emerged as powerful tools in scientific computing, offering new ways to approximate solutions to problems traditionally addressed by numerical methods. While classical techniques such as finite difference, finite element, and Runge-Kutta methods remain foundational for solving differential equations, neural networks provide a mesh-free, data-driven alternative that may generalize better in certain contexts.

This report investigates the viability of neural networks for approximating solutions to differential equations. Rather than comparing these methods directly with classical techniques, we focus on evaluating their performance across a range of problem types, and on identifying how their effectiveness depends on architectural choices. Specifically, we consider their application to ordinary differential equations (ODEs), including initial value problems (IVPs) and boundary value problems (BVPs). We examine their ability to interpolate and extrapolate various types of solutions — including exponential decay, oscillatory behaviour, and singularities. As an extension, we also investigate the use of neural networks in solving selected partial differential equations (PDEs) using similar criteria. In each case, we analyse how performance varies with different network architectures and activation functions.

This report is structured as follows:

- **Section 2** introduces the core concepts of neural networks, including their architecture and training via backpropagation. It then outlines the specifics of using neural networks to solve differential equations, illustrating the methodology with a simple example.
- **Section 3** explores the use of neural networks for solving ODEs, dividing the discussion into IVPs and BVPs. For each, we examine a range of representative problems and analyse networks' ability to capture the underlying solution behaviour, and how that ability varies with architecture and activation function choices.
- **Section 4** extends the investigation to PDEs, following a similar approach. We test the network on a simple problem and assess how well they satisfy the relevant constraints.
- **Section 5** concludes the report by summarising the findings and suggesting directions for further study.

2 Preliminaries

In this section, we outline the basic setup, components, and architecture of feedforward neural networks, and describe the standard approach used for training them. While multiple types of neural networks exist (e.g., convolutional neural networks, recurrent neural networks), we restrict our attention to feedforward neural networks. All references to neural networks in this report refer exclusively to this type.

Throughout, we adopt the following notation: vectors are denoted using lowercase bold symbols (e.g., $\mathbf{x}$), while matrices are written in uppercase bold (e.g., $\mathbf{W}$). We denote the output of the neural network as $\hat{y}$, which approximates a target function y.

2.1 Neural Networks Overview and Architecture

A feedforward neural network defines a function $f_\theta : \mathbb{R}^n \to \mathbb{R}^m$, parameterised by a collection of weight matrices and bias vectors $\theta = \{\mathbf{W}^{(l)}, \mathbf{b}^{(l)}\}_{l=1}^{L}$. It is trained to approximate a target function $y : \mathbb{R}^n \to \mathbb{R}^m$ using observed or synthetically generated data.

The model takes an input vector $\mathbf{x} \in \mathbb{R}^n$ and propagates it forward through a sequence of L layers, each composed of individual units called *neurons*.

Each neuron in a given layer, l, performs a simple two-step operation. First, it computes a weighted sum of its inputs and adds a bias term. Then, it applies a non-linear activation function to the result. Specifically, if a neuron with weights $\mathbf{w}_i^{(l)} \in \mathbb{R}^{n_{l-1}}$ and bias $b_i^{(l)} \in \mathbb{R}$ receives an input vector $\mathbf{z}^{(l-1)} \in \mathbb{R}^{n_{l-1}}$, then its output is given by

$$z_i^{(l)} = \sigma\left((\mathbf{w}_i^{(l)})^\top \mathbf{z}^{(l-1)} + b_i^{(l)}\right),$$

where $\sigma : \mathbb{R} \to \mathbb{R}$ is the neuron's fixed activation function.

A layer consists of multiple such neurons, all operating in parallel on the same input vector $\mathbf{z}^{(l-1)}$, each with its own weight vector and bias. The outputs from all neurons in the layer are collected into a vector $\mathbf{z}^{(l)} \in \mathbb{R}^{n_l}$, where n_l denotes the number of neurons in layer l. Letting $\mathbf{W}^{(l)} \in \mathbb{R}^{n_l \times n_{l-1}}$ be the matrix whose rows are the individual neuron weight vectors $(\mathbf{w}_i^{(l)})^\top$, and $\mathbf{b}^{(l)} \in \mathbb{R}^{n_l}$ the vector of biases, we can express the full layer computation compactly as

$$\mathbf{z}^{(l)} = \sigma\left(\mathbf{W}^{(l)}\mathbf{z}^{(l-1)} + \mathbf{b}^{(l)}\right),$$

with the activation function σ now applied componentwise.

The network as a whole consists of a composition of such layers. Starting from the input vector $\mathbf{z}^{(0)} = \mathbf{x}$, each successive layer transforms the output of the previous one. For a network with L layers, the computation proceeds recursively:

$$\mathbf{z}^{(l)} = \sigma^{(l)}\left(\mathbf{W}^{(l)}\mathbf{z}^{(l-1)} + \mathbf{b}^{(l)}\right), \quad \text{for } l = 1, \ldots, L-1,$$

with the final output given by

$$\hat{\mathbf{y}} = f_\theta(\mathbf{x}) = \sigma^{(L)}(\mathbf{W}^{(L)}\mathbf{z}^{(L-1)} + \mathbf{b}^{(L)}).$$

The total set of network parameters $\theta = \{\mathbf{W}^{(l)}, \mathbf{b}^{(l)}\}_{l=1}^{L}$ are learned during training. The architecture is defined by the number of layers L (often referred to as the *depth* of the network), the number of neurons n_l in each layer (also referred to as the *depth*), and the choice of activation functions $\sigma^{(l)}$. The first and last layers are termed the input and output layers respectively, while intermediate layers are termed hidden layers [1]. Figure 1 gives an an illustrative diagram of a neural network architecture, with each neuron denoted by a circle, and connections indicating the output of one neuron passed as an input to neurons in the next layer.

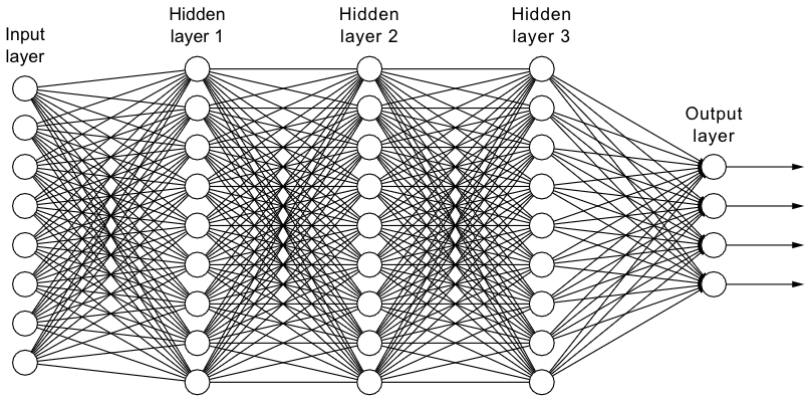

Figure 1: Illustration of a fully connected feedforward neural network with three hidden layers. Each neuron computes an affine transformation of its inputs followed by a non-linear activation.

Common activation functions used include:

- **Hyperbolic tangent (tanh):** $\sigma(x) = \tanh(x) = \dfrac{e^x - e^{-x}}{e^x + e^{-x}}$
- **Rectified Linear Unit (ReLU):** $\sigma(x) = \max(0, x)$
- **Leaky ReLU:** $\sigma(x) = \begin{cases} x, & \text{if } x \geq 0 \\ \alpha x, & \text{if } x < 0 \end{cases}$, for small $\alpha > 0$.

- **Sinusoidal:** $\sigma(x) = \sin(x)$,

In this report we will restrict ourselves to considering these activation functions.

2.2 Training

The parameters of a neural network — namely the weight matrices and bias vectors $\theta = \{\mathbf{W}^{(l)}, \mathbf{b}^{(l)}\}_{l=1}^{L}$ — are learned through a process called *training*. The goal of training is to find a parameter set θ^* such that the network output $\hat{y} = f_{\theta^*}(\mathbf{x})$ closely approximates the desired output y over a set of inputs $\mathbf{x} \in \mathbb{R}^n$.

This is accomplished by defining a *loss function* $\mathcal{L}(\theta)$ that quantifies the discrepancy between the network predictions and the target values across a training dataset. In this way, training becomes a minimisation problem, where the goal is to find the parameter configuration θ^* that minimises the loss function $\mathcal{L}$. When the desired outputs are continuous, a common choice is the mean squared error (MSE):

$$\mathcal{L}(\theta) = \frac{1}{N} \sum_{i=1}^{N} \left\| f_\theta(\mathbf{x}^{(i)}) - y^{(i)} \right\|^2,$$

where $\{(\mathbf{x}^{(i)}, y^{(i)})\}_{i=1}^{N}$ is the training dataset of input-output pairs.

To minimise the loss function, $\mathcal{L}(\theta)$, a gradient-based optimisation method is used. This requires computing the gradient of the loss with respect to all network parameters. This is made efficient by the *backpropagation algorithm*, which systematically applies the chain rule of calculus to compute these derivatives by propagating error signals backward through the layers of the network.

Let us denote the output of layer l as $\mathbf{z}^{(l)} \in \mathbb{R}^{n_l}$, computed via

$$\mathbf{z}^{(l)} = \sigma^{(l)}\left(\mathbf{a}^{(l)}\right), \quad \text{where} \quad \mathbf{a}^{(l)} = \mathbf{W}^{(l)}\mathbf{z}^{(l-1)} + \mathbf{b}^{(l)},$$

and $\sigma^{(l)}$ is the activation function applied componentwise.

Define the error signal at layer l as

$$\boldsymbol{\delta}^{(l)} := \frac{\partial \mathcal{L}}{\partial \mathbf{a}^{(l)}},$$

which captures the sensitivity of the loss to the pre-activation input at that layer. The error at the final layer L is computed using the derivative of the loss function with respect to the network output:

$$\boldsymbol{\delta}^{(L)} = \nabla_{\hat{\mathbf{y}}} \mathcal{L} \odot \sigma'^{(L)}\left(\mathbf{a}^{(L)}\right),$$

where $\odot$ denotes elementwise (Hadamard) product and $\sigma'^{(L)}$ is the derivative of the activation function at the final layer.

For hidden layers $l = L-1, \ldots, 1$, the errors are computed recursively using

$$\boldsymbol{\delta}^{(l)} = \left((\mathbf{W}^{(l+1)})^\top \boldsymbol{\delta}^{(l+1)} \right) \odot \sigma'^{(l)} \left(\mathbf{a}^{(l)} \right).$$

Once the error signals are computed for each layer, the gradients of the loss with respect to the weights and biases are given by

$$\frac{\partial \mathcal{L}}{\partial \mathbf{W}^{(l)}} = \boldsymbol{\delta}^{(l)} (\mathbf{z}^{(l-1)})^\top, \quad \frac{\partial \mathcal{L}}{\partial \mathbf{b}^{(l)}} = \boldsymbol{\delta}^{(l)}.$$

These gradients are then used in an optimisation routine, such as Adam or Stochastic Gradient Descent, to update the parameters:

$$\mathbf{W}^{(l)} \leftarrow \mathbf{W}^{(l)} - \alpha \frac{\partial \mathcal{L}}{\partial \mathbf{W}^{(l)}}, \quad \mathbf{b}^{(l)} \leftarrow \mathbf{b}^{(l)} - \alpha \frac{\partial \mathcal{L}}{\partial \mathbf{b}^{(l)}},$$

where $\alpha > 0$ is a hyperparameter termed the learning rate.

This optimisation process is repeated over the training dataset in multiple passes (epochs), until convergence to a local minimum of the loss function.

This iterative update process constitutes the core of neural network training, and naturally divides the procedure into a sequence of *forward passes*, where predictions are computed by modifying and propagating forward the inputs, and *backward passes*, where gradients are propagated backwards and parameters are updated. Each training epoch can be visualised as a forward sweep through the network architecture, illustrated by Figure 1, that generates outputs, followed by a backward sweep in which gradients are computed via backpropagation and used to adjust the network parameters.

2.3 Neural Networks for Differential Equations

When applying neural networks to solve differential equations, the nature of the problem differs fundamentally from standard supervised learning tasks. In conventional machine learning, a model learns from a dataset of labelled input-output pairs $\{(\mathbf{x}^{(i)}, y^{(i)})\}$, and is trained to minimise prediction error on unseen examples drawn from the same underlying distribution. In contrast, solving a differential equation involves finding a function that satisfies a differential constraint and associated boundary or initial conditions. No explicit data labels are given; instead, a loss function is constructed that penalises violations of the governing equation at selected collocation points. This loss typically involves computing derivatives of the network output

with respect to its input — a task well suited to modern automatic differentiation frameworks.

Another key difference is that supervised learning often involves noisy training data due to measurement error or system variability. Neural networks in that context are trained to generalise despite this uncertainty. Differential equation problems, by contrast, are typically deterministic: the equations are known exactly, and the solution is expected to satisfy them precisely. As a result, the concepts of overfitting and underfitting take on new meaning, referring to how well the learned function satisfies the equation and constraints, rather than its generalisation to unseen data.

Before analysing more complex problem classes, we conclude this section with a simple illustrative example. This serves to demonstrate the methodology outlined, reinforce the distinctions from standard supervised learning highlighted above, and validate our implementation method. It is also representative of the general method applied in subsequent sections when training neural networks in this report.

We consider the boundary value problem

$$\begin{aligned} y''(x) &= 2, \quad 0 < x < 1, \\ y(0) &= 1, \\ y(1) &= 1, \end{aligned}$$

whose exact solution is $y(x) = 1 + x(1 - x)$.

We approximate this solution using a neural network $\hat{y}(x) = f_\theta(x)$, where θ denotes the trainable weights and biases. The loss function penalises both deviations from the differential equation and violations of the boundary conditions:

$$\mathcal{L}(\theta) = \sum_{k=1}^{N} \left(\hat{y}''(x_k) - 2\right)^2 + \gamma \left(\hat{y}(0) - 1\right)^2 + \gamma \left(\hat{y}(1) - 1\right)^2, \tag{1}$$

where $\{x_k\}_{k=1}^N \subset (0, 1)$ are collocation points. $\gamma > 0$ is another hyperparameter that functions as a penalty coefficient, scaling the importance of $f_\theta(x)$ satisfying the boundary conditions relative to satisfying the governing equation.

The model architecture we use to solve this problem is illustrated in Figure 2. It consists of a fully connected feedforward neural network with two hidden layers, each containing five neurons. The activation function in the hidden layers is the hyperbolic tangent, $\tanh(x)$, chosen for its smoothness and differentiability. No activation is used in the output layer, consistent with regression tasks involving continuous outputs [1].

The network is trained on 20 equally spaced points in $[0, 1]$, including the boundary values at $x = 0$ and $x = 1$. We set $\gamma = 1$ in the loss function (1), and optimise using

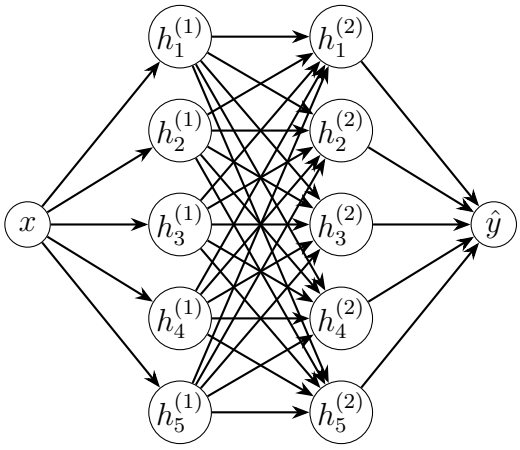

Figure 2: Fully connected feedforward neural network used to approximate the solution $\hat{y}(x)$. The network takes a scalar input x, passes it through two hidden layers with five neurons each, and outputs a scalar prediction.

the Adam algorithm with a fixed learning rate of $\alpha = 0.001$. Training proceeds for 2000 epochs.

Figure 3 shows the training diagnostics. The left panel illustrates the convergence of the loss during training. The right panel compares the network's prediction to the true solution. The neural network recovers the solution accurately across the domain, with minor deviations near the centre. By increasing the number of epochs we would likely have further have further reduced these deviations.

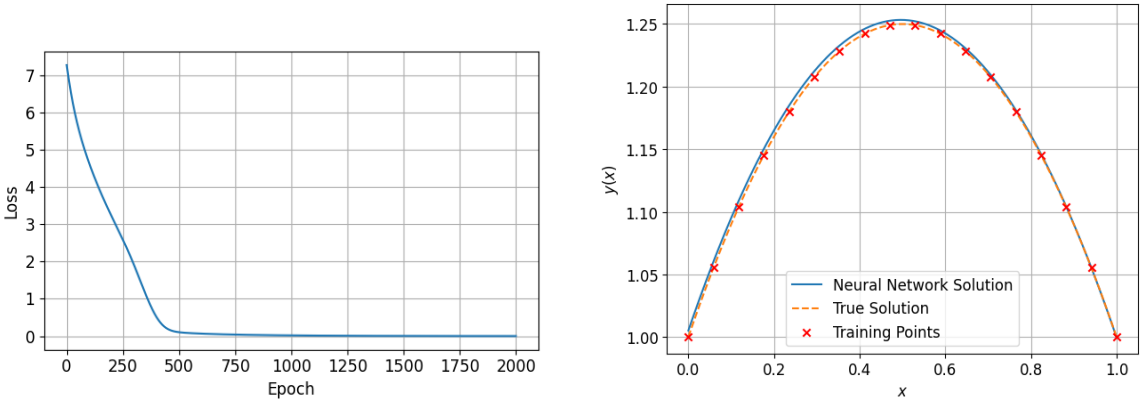

(a) Training loss over 2000 epochs.

(b) Neural network prediction vs true solution.

Figure 3: Training diagnostics for the neural network solution to the ODE.

3 Ordinary Differential Equations

Having outlined the methodology for using neural networks to solve differential equations, in this section we begin a more systematic investigation of their performance across a range of ordinary differential equation (ODE) problems. This section is divided into two main parts: initial value problems (IVPs) and boundary value problems (BVPs). In each case, we examine the extent to which neural networks can learn accurate solutions, and how their performance is affected by architectural choices.

In the IVP setting, we consider three representative classes of problems: exponential decay, solutions exhibiting a singularity, and periodic solutions. These problems allow us to assess both interpolation accuracy and a network's ability to extrapolate beyond the training domain.

For BVPs, our focus will remain on evaluating the quality of the approximation within the prescribed domain. Since boundary conditions are enforced at fixed endpoints, extrapolation beyond the interval is not typically meaningful. Instead, we investigate how the network adapts to constraints at both boundaries, and how well it captures internal behaviour with different choices of architecture and optimisation.

To systematically explore the influence of key design parameters we will vary: the number of neurons per hidden layer, the number of hidden layers and the choice of activation function. These experiments will serve to assess neural networks ablity to solve differential equation problems, along with understanding how this ability varies with architectural choices. We do not consider networks with different numbers of neurons in each layer, and we use the MSE loss function for all models.

We deliberately restrict our investigation to variations in network architecture and activation functions, holding other hyperparameters fixed (such as the learning rate, optimiser type, and penalty parameters for enforcing boundary conditions). This choice simplifies the analysis and enables clearer interpretation of the results by isolating the effects of architectural design. Our primary interest lies in the representational capability of neural networks — that is, how well different architectures can approximate solutions once trained — rather than in training efficiency. Provided that convergence is achieved, changes to hyperparameters like the learning rate or penalty weight primarily influence the speed or stability of training, not the final quality of the fit. To this end, we use the Adam optimiser, which is widely regarded as robust to hyperparameter settings such as the learning rate and penalty weight ([1], Section 8.5.4). To ensure fairness and comparability, all models were trained for the same number of epochs (typically 2500). A learning rate $\alpha = 0.001$ and penalty

weight $\gamma = 100$ was used, and solutions examined to ensure convegrence was observed. All models were implemented in python using the python library PyTorch [2].

3.1 Initial Value Problems

Exponential Decay We begin with a simple initial value problem whose solution exhibits exponential decay:

$$y'(x) = -y(x)$$
$$y(0) = 1.$$

This has exact solution $y(x) = e^{-x}$, which is smooth, bounded, and monotonically decreasing. This problem serves as a useful baseline for evaluating the ability of neural networks to approximate well-behaved solutions over a finite interval and extrapolate beyond.

To investigate the impact of network architecture, we train a family of feedforward neural networks with varying depth and width. Specifically, we fix the optimiser (Adam) and learning rate, and systematically vary the number of hidden layers (from 1 to 10) and the number of neurons per layer (from 1 to 20). For each configuration, we evaluate the mean squared error (MSE) between the network prediction and the true solution on a uniform grid of evaluation points. This procedure is repeated for two different sets of activation functions: tanh and ReLU.

The heatmaps in Figure 4 reveal several consistent trends. For both activation functions, increasing the number of neurons per layer generally leads to improved accuracy for a fixed number of layers. In contrast, increasing depth alone does not guarantee better performance, particularly when layers are narrow. The best-performing configurations are found with moderately deep networks (4–8 layers) and wider layers (10–20 neurons), though the overall sensitivity to architecture is relatively mild — likely due to the simplicity of the target function. More striking differences emerge in extrapolation. The ReLU-based networks fail to capture the exponential decay beyond the training domain, typically reverting to a linear trajectory. By contrast, the networks trained with tanh not only interpolate more accurately but also exhibit qualitatively correct exponential behaviour when extrapolated to $x = 10$. Notably, the best tanh network also performs well in the extrapolated region, while the worst-fitting example remains poor throughout. Finally, we observe in our heatmap that the error for most neural network architectures using the tanh activation function has lower MSE than those using the ReLu function.

Periodic Solution We now consider an initial value problem whose solution is periodic:

$$y'(x) = \cos x,$$
$$y(0) = 0.$$

The exact solution is $y(x) = \sin x$, which is smooth, bounded, and periodic with period 2π. This problem allows us to evaluate the capacity of neural networks to approximate oscillatory behaviour across a wide domain, and to test whether the learned solution generalises beyond a single period.

We perform the same analysis as in the previous section, first analysing how the error varies for different architectures, and then examining best solutions (we exclude the worst cases now, as these were purely for comparison to best in the preceding section), shown in Figure 6.

We first observe that the neural networks using the tanh activation function are clearly more successful at solving this particular solution, almost entirely failing to....

Singular Solution We now turn to an initial value problem whose solution contains a singularity:

$$y'(x) = y(x)^2,$$
$$y(0) = 1,$$
$$y(1.05) = -20$$

The exact solution is $y(x) = \frac{1}{1-x}$, which becomes singular at $x = 1$. This problem is useful for testing the ability of neural networks to approximate rapidly varying functions and to capture solution blow-up within a finite domain.

To mitigate instability near the singularity, we train two separate networks: one on the interval $[0, 0.95]$ using the initial condition $y(0) = 1$, and one on the interval $[1.05, 2.0]$ using the analytically derived condition $y(1.05) = -20$. This approach allows us to evaluate how well neural networks can approximate the solution on either side of the singularity without numerical breakdown.

3.2 Boundary Value Problems

We now consider boundary value problems (BVPs), where the solution is defined by a differential equation along with prescribed values at the boundaries of a fixed domain. Unlike initial value problems, BVPs specify constraints at multiple points—typically at the endpoints of an interval—and the solution must satisfy the differential equation throughout the domain while adhering to these boundary conditions.

In this section, we investigate how well neural networks can approximate solutions to BVPs using the same methodology outlined for IVPs. However, since BVPs are defined strictly on a bounded interval, we do not consider extrapolation performance here. Instead, we focus on how accurately the networks capture the solution within the specified domain.

We consider two representative BVPs:

- A smooth Poisson-type problem, with known analytic solution $y(x) = sin(\pi x)$, serving as a baseline.
- A piecewise forcing problem with a discontinuous right-hand side, used to examine network behaviour under more challenging conditions.

For each problem, we evaluate neural network performance across a range of architectures and activation functions, using mean squared error (MSE) as the primary metric. Heatmaps and example fits are used to visualise how architectural choices affect solution quality.

Poisson Problem We begin with a classical boundary value problem from mathematical physics:

$$\begin{aligned} -y''(x) &= \pi^2 \sin(\pi x), \quad x \in (0,1), \\ y(0) &= 0, \\ y(1) &= 0. \end{aligned}$$

This has the exact solution $y(x) = \sin(\pi x)$, which is smooth, bounded, and vanishes at both endpoints. The problem provides a simple but instructive setting to evaluate how well neural networks approximate solutions to second-order differential equations with smooth forcing and well-defined boundary conditions.

As in the IVP analysis, we assess the effect of architectural variation on solution accuracy. For each combination of depth, width, and activation function, we compute the MSE across the domain, and visualise the results using heatmaps and representative fits. The best solutions are shown in Figure 7.

Piecewise Forcing We now consider a boundary value problem with a discontinuous right-hand side:

$$y''(x) = \begin{cases} -1, & 0 \leq x < 0.5, \\ +1, & 0.5 \leq x \leq 1, \end{cases}$$
$$y(0) = 0,$$
$$y(1) = 0.$$

This problem admits a piecewise quadratic solution that is continuous and satisfies the boundary conditions. However, the discontinuity in the forcing term results in a derivative jump at $x = 0.5$, which poses a challenge for smooth neural network approximators.

This example allows us to assess how well neural networks can resolve low-regularity features in the solution and adapt to discontinuous dynamics in the governing equation. As before, we systematically vary network architecture and activation function, compute the corresponding approximation error, and visualise representative results. The best-fitting solutions are summarised in Figure 8.

4 Extension: Partial Differential Equations

5 Conclusion

References

[1] Ian Goodfellow et al. *Deep learning*. Vol. 1. 2. MIT press Cambridge, 2016.

[2] Adam Paszke et al. "Automatic differentiation in PyTorch". In: (2017).

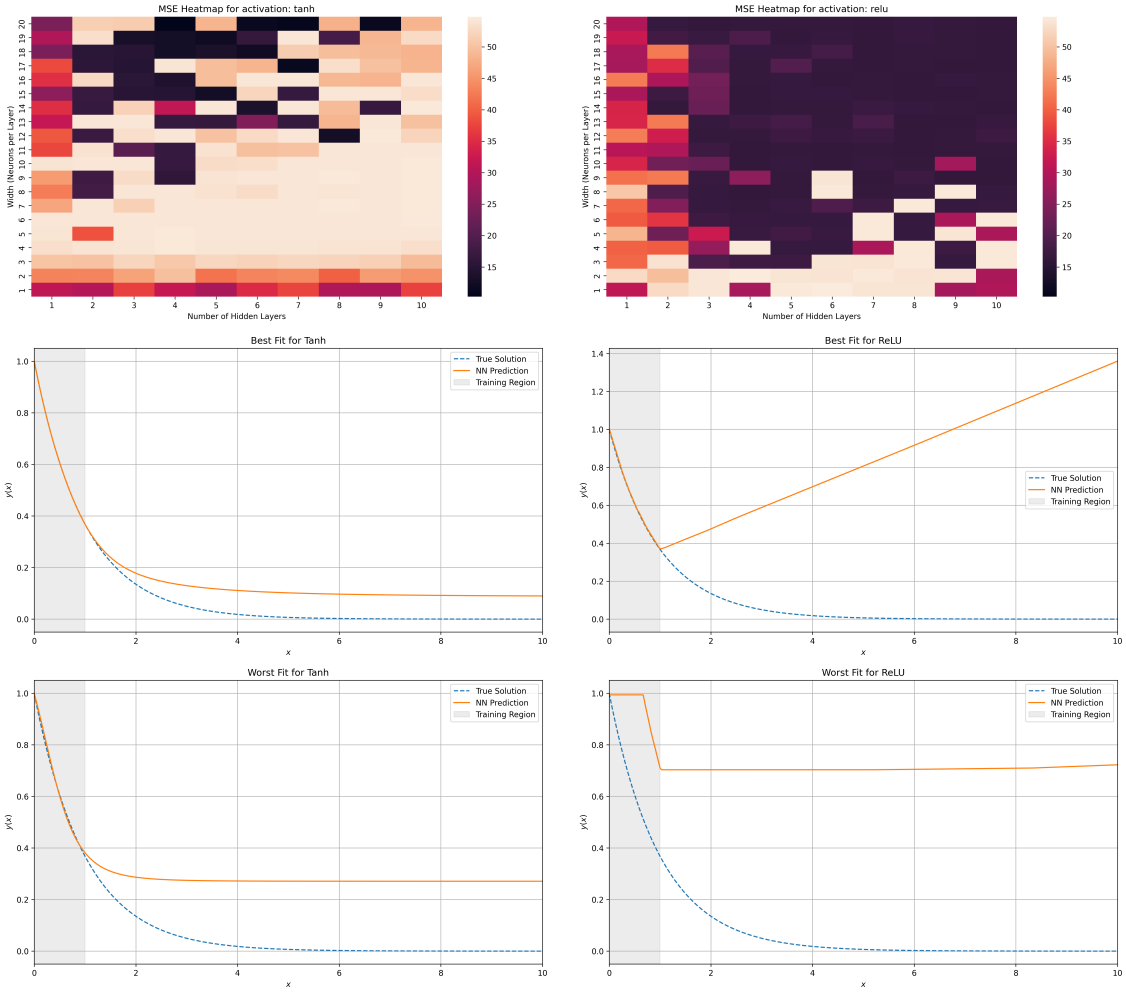

(a) **Tanh activation.** Heatmap (top), best fit (middle), and worst fit (bottom).

(b) **ReLU activation.** Heatmap (top), best fit (middle), and worst fit (bottom).

Figure 4: Comparison of architectural performance for the exponential decay problem using two activation functions. Each column shows the MSE heatmap with a log error scale, the best network fit, and the worst network fit.

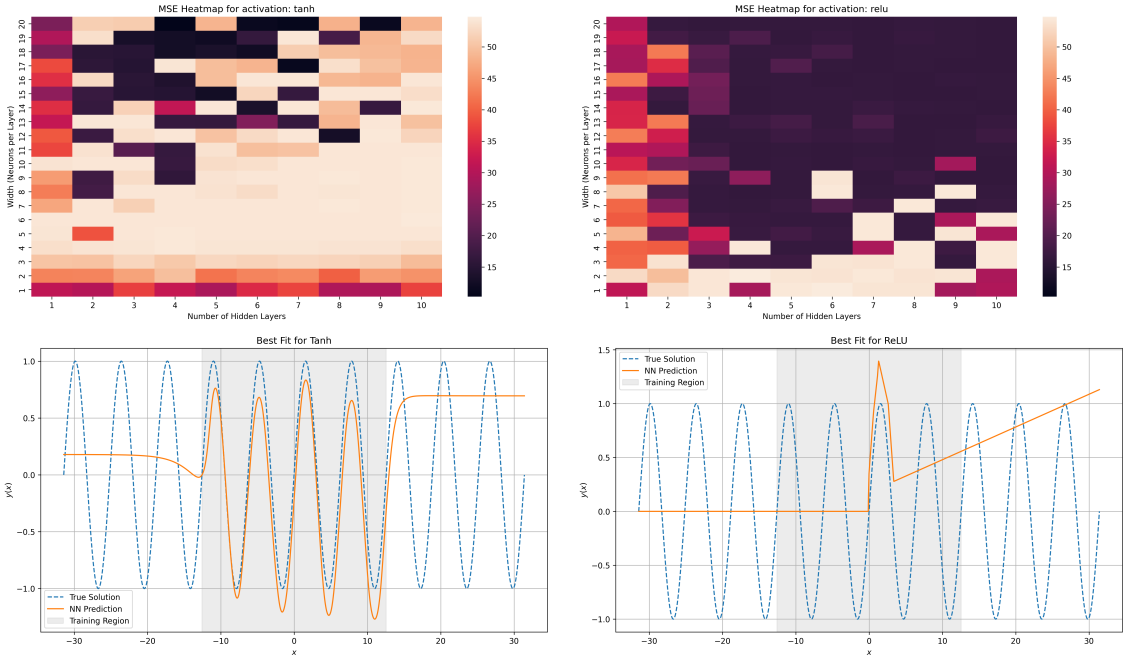

(a) **Tanh activation.** Heatmap (top), best fit (middle), and worst fit (bottom).

(b) **ReLU activation.** Heatmap (top), best fit (middle), and worst fit (bottom).

Figure 5: Comparison of architectural performance for the exponential decay problem using two activation functions. Each column shows the MSE heatmap with a log error scale, the best network fit, and the worst network fit.

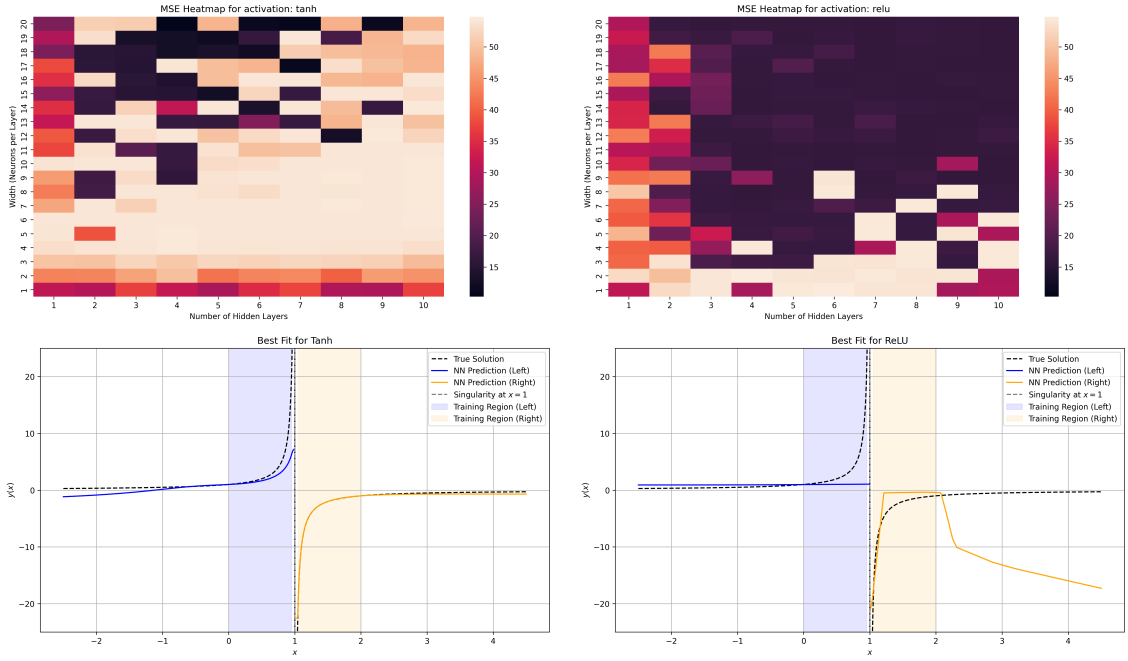

(a) **Tanh activation.** Heatmap (top), best fit (middle), and worst fit (bottom).

(b) **ReLU activation.** Heatmap (top), best fit (middle), and worst fit (bottom).

Figure 6: Comparison of architectural performance for the exponential decay problem using two activation functions. Each column shows the MSE heatmap with a log error scale, the best network fit, and the worst network fit.

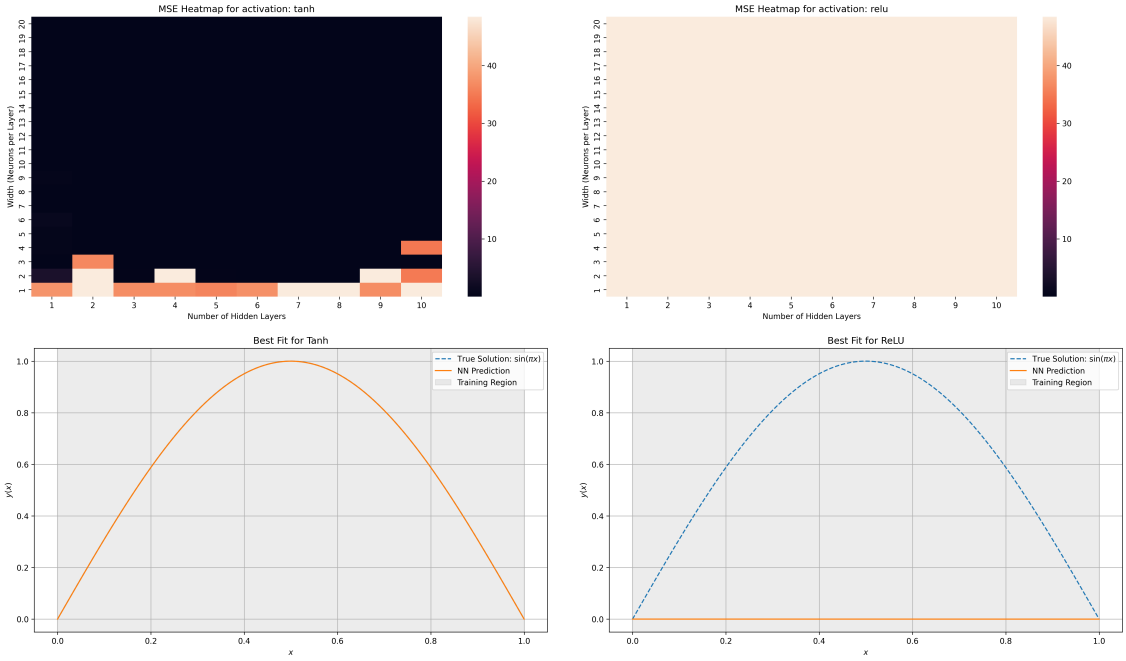

(a) **Tanh activation.** Heatmap (top), best fit (middle), and worst fit (bottom).

(b) **ReLU activation.** Heatmap (top), best fit (middle), and worst fit (bottom).

Figure 7: Comparison of architectural performance for the exponential decay problem using two activation functions. Each column shows the MSE heatmap with a log error scale, the best network fit, and the worst network fit.

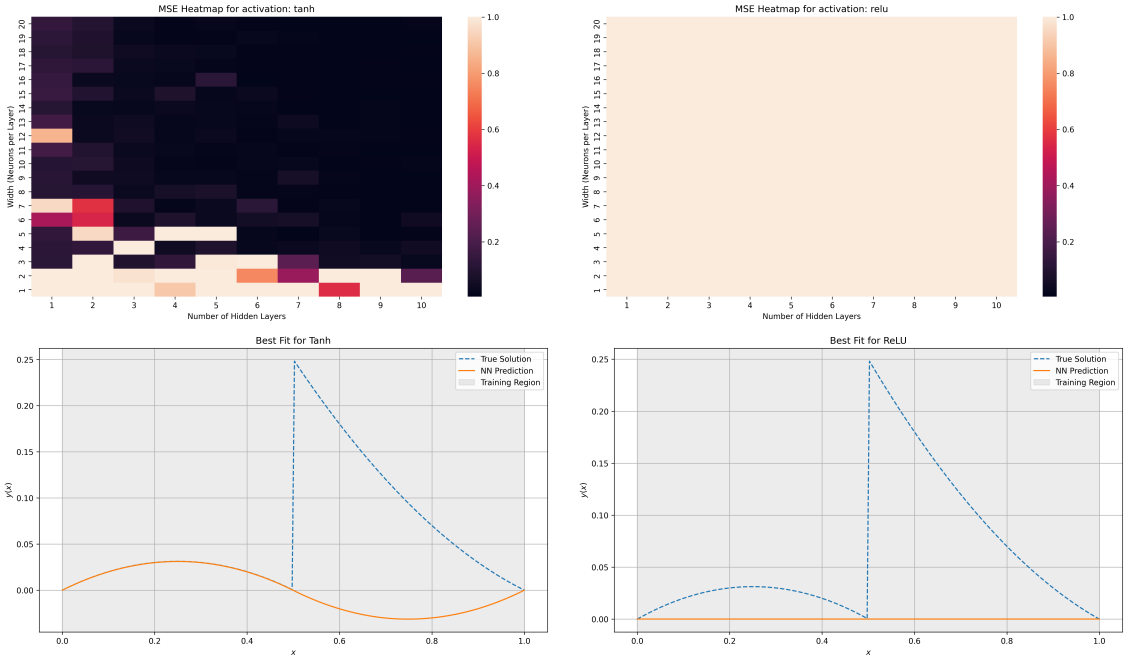

(a) **Tanh activation.** Heatmap (top), best fit (middle), and worst fit (bottom).

(b) **ReLU activation.** Heatmap (top), best fit (middle), and worst fit (bottom).

Figure 8: Comparison of architectural performance for the exponential decay problem using two activation functions. Each column shows the MSE heatmap with a log error scale, the best network fit, and the worst network fit.